

CHALMERS | GÖTEBORG UNIVERSITY

PREPRINT 2006:22

Multigrid for Quadratic Finite Elements

ERIK D. SVENSSON

*Department of Mathematical Sciences
Division of Mathematics*

**CHALMERS UNIVERSITY OF TECHNOLOGY
GÖTEBORG UNIVERSITY
Göteborg Sweden 2006**

Preprint 2006:22

Multigrid for Quadratic Finite Elements

Erik D. Svensson

CHALMERS | GÖTEBORG UNIVERSITY



Department of Mathematical Sciences
Division of Mathematics
Chalmers University of Technology and Göteborg University
SE-412 96 Göteborg, Sweden
Göteborg, August 2006

Preprint 2006:22
ISSN 1652-9715

Matematiska vetenskaper
Göteborg 2006

MULTIGRID FOR QUADRATIC FINITE ELEMENTS

ERIK D. SVENSSON

ABSTRACT. We investigate the convergence rate of the finite element multigrid method applied on quadratic finite element approximations for problems with full and less than full regularity.

1. INTRODUCTION

The finite element multigrid method solves linear systems of equations arising from finite element approximations to linear elliptic partial differential equations with a number of operations proportional to the number of unknowns. We say that the multigrid method has optimal complexity or scales optimally. The method is founded on solid theoretical results which are reviewed in for example [7, 13, 21]. However, it is important to note that this rather general statement is really limited to linear finite element approximations. For higher degree finite element approximations the convergence rate of the multigrid method may deteriorate see, for example, [16] and for the similar problem for the algebraic multigrid method [14].

On the other hand, for sufficiently smooth problems and for finite element approximations of degree $q > 1$ we may achieve $O(h^{q+1})$ convergence in the error $u - u_h$, measured in some suitable norm, where h is the mesh size and, u and u_h are the exact and the finite element solutions, respectively. This is appealing and motivate us to study multigrid solvers for higher degree approximations. Moreover, there are situations that for other reasons require higher degree approximations, for example, solving saddle point problems such as the Stokes equations using the Hood-Taylor finite elements.

In this work we demonstrate that the multigrid method in practice also works well for quadratic finite element approximations of problems with

Date: April 19, 2006.

2000 Mathematics Subject Classification. 65N55, 65N30.

Key words and phrases. multigrid, finite elements.

both full regularity and less than full regularity. We compare two different finite element approximations, the Lagrange approximation and the quadratic hierarchical approximation studied in [2], originally suggested in [3]. We use the general theory outlined in [7] to indicate how the point Gauss-Seidel smoother deteriorates as a function of the dimension n of the problem and the degree q of the approximation.

We found only a few references in the literature on multigrid methods for higher degree finite elements. For example in the monograph [7] a general theory is presented although only linear finite elements are considered explicitly.

1.1. Preliminaries. We assume the underlying problem is a second order linear elliptic equation on a polyhedral domain $\Omega \subset \mathbf{R}^n$ for $n = 2, 3$. Let $a(\cdot, \cdot) : V \times V \rightarrow \mathbf{R}$ be a continuous symmetric V -elliptic bilinear form, and let $f(\cdot) : V \rightarrow \mathbf{R}$ be a continuous linear form. We pose the problem in general form and consider the variational formulation

$$(1.1) \quad u \in V : \quad a(u, v) = f(v) \quad \forall v \in V,$$

where we assume that $V \subset H^1(\Omega)$ is a Hilbert space such that (1.1) is well-posed.

For any measurable set $\omega \subseteq \mathbf{R}^n$, $n = 2, 3$, let $|\omega|$ denoted its measure. We will use standard notation for the Lebesgue and Sobolev spaces with corresponding norms

$$\|\cdot\|_{L^2(\omega)} = \|\cdot\|_{0,\omega} \quad \text{and} \quad \|\cdot\|_{H^s(\omega)} = \|\cdot\|_{s,\omega},$$

and when $\omega = \Omega$, and it is clear from the context, we will simplify the notation and write

$$\|\cdot\|_{0,\Omega} = \|\cdot\|_0 \quad \text{and} \quad \|\cdot\|_{s,\Omega} = \|\cdot\|_s,$$

and likewise for the $L^2(\omega)$ scalar product

$$(u, v)_\omega = \int_\omega uv \, dx,$$

see, for example, [1] for more details.

We also use the norm defined by

$$\|v\| = a(v, v)^{1/2} \quad \forall v \in V.$$

For vectors $\tilde{v} = (\tilde{v}_1, \dots, \tilde{v}_N) \in \mathbf{R}^N$ we will use the Euclidean norm denoted by $\|\tilde{v}\| = (\tilde{v}_1^2 + \tilde{v}_2^2 + \dots + \tilde{v}_N^2)^{1/2}$.

Finally, throughout this work we will use C and c_i to denote various constants, not necessarily taking the same values from time to time.

1.2. Finite elements. We will use the notion *finite element* to denote the triplets $(T, \mathcal{P}, \mathcal{N})$ where $T \subset \Omega$ is a non-empty Lipschitz continuous set, \mathcal{P} is a finite dimensional space of functions on T and $\mathcal{N} = \{N_1, N_2, \dots, N_{m_q}\}$ is a basis for \mathcal{P}' , the set of nodal variables [8, 9].

As for T we only consider n -simplices with vertices $a_i \in \mathbf{R}^n$ for $i = 1, \dots, n+1$ and $n = 2, 3$ as in Figure 1.1 and 1.2a. We set $h_T = \text{diam}(T)$.

Let \mathcal{P}_q to denote the space of polynomials of degree $\leq q$ and note that

$$(1.2) \quad \dim \mathcal{P}_q = \binom{n+q}{q} = \text{card}(\mathcal{N}) = m_q,$$

where we use the cardinal number to count the number of elements in a set.

Let $L_q(T)$ denote the *principal lattice of order q* on T with m_q lattice points [9, Theorem 6.1, p. 70], that is,

$$L_q(T) = \left\{ x = \sum_{i=1}^{n+1} \xi_i a_i : \sum_{i=1}^{n+1} \xi_i = 1, \xi_i \in \left\{ 0, \frac{1}{q}, \dots, \frac{q-1}{q}, 1 \right\} \right\}$$

For example, $L_1(T) = \{a_i\}_{i=1}^{n+1}$ is the set of vertices of the n -simplex T , and $L_2(T) = \{a_i\}_{i=1}^{n+1} \cup \{a_{ij} = (a_i + a_j)/2 : 1 \leq i < j \leq n+1\}$, see Figures 1.1 and 1.2a.

We use the common practice and refer to points in $L_q(T)$ as *local nodes*.

In order to express \mathcal{P}_q we use *barycentric coordinates* on T , that is, the functions $\lambda_i \in \mathcal{P}_1$ such that $\lambda_i(a_j) = \delta_{ij}$ for $a_j \in L_1(T)$ and $i, j = 1, \dots, n+1$, see, for example [11].

Given a basis $\{N_1, N_2, \dots, N_{m_q}\}$ to \mathcal{P}'_q we choose a basis $\{\varphi_1, \varphi_2, \dots, \varphi_{m_q}\}$ to \mathcal{P}_q so that $N_i(\varphi_j) = \delta_{ij}$ for $i, j = 1, \dots, m_q$.

Let $(\widehat{T}, \widehat{\mathcal{P}}, \widehat{\mathcal{N}})$ denote the reference finite element where \widehat{T} is either the triangle with vertices in $(0, 0), (1, 0), (0, 1)$ or the tetrahedron with vertices in $(0, 0, 0), (1, 0, 0), (0, 1, 0), (0, 0, 1)$. We will assume that all finite elements $(T, \mathcal{P}, \mathcal{N})$ are equivalent to the reference finite element. Thus, there is an invertible affine mapping

$$(1.3) \quad F : \mathbf{R}^n \ni x \longmapsto F(x) = Bx + b \in \mathbf{R}^n$$

such that $F(\widehat{T}) = T$, $F^*\widehat{\mathcal{P}} = \mathcal{P}$ and $F_*\widehat{\mathcal{N}} = \mathcal{N}$ where F^* and F_* denote the pull-back and push-forward operators, see [8].

1.2.1. *Lagrange finite elements.* We recall the definition of the standard Lagrange finite element which determines a finite element space of continuous piecewise polynomials of degree $q \geq 1$. In terms of the triplet $(T, \mathcal{P}, \mathcal{N})$, $\mathcal{P} = \mathcal{P}_q$ with basis functions $\varphi_i \in \mathcal{P}_q$ for $i = 1, \dots, m_q$ such that $\varphi_i(x_j) = \delta_{ij}$ and the nodal variables are defined by $N_j(v) = v(x_j)$ for $x_j \in L_q(T)$ and $v \in C^0$. For example: if $q = 1$, $\varphi_i = \lambda_i$, and if $q = 2$, $\varphi_i = \lambda_i(2\lambda_i - 1)$ for $i = 1, \dots, n+1$, and $\varphi_{ij} = 4\lambda_i\lambda_j$ for $1 \leq i < j \leq n+1$ denoting the last $n+2, \dots, m_2$ basis functions.

1.2.2. *Higher degree hierarchical finite elements.* We consider the higher degree hierarchical finite element which determines a finite element spaces of continuous piecewise polynomials of degree $q \geq 2$ as outlined in [2]. In terms of the triplet $(T, \mathcal{P}, \mathcal{N})$, $\mathcal{P} = \mathcal{P}_1 \oplus \mathcal{B}_q$ where \mathcal{B}_q is the space of polynomials of degree > 1 and $\leq q$, that is, excluding the linear polynomials. For example: if $q = 2$, we choose $\varphi_i = \lambda_i$ for $i = 1, \dots, n+1$, and $\varphi_{ij} = 4\lambda_i\lambda_j$ for $1 \leq i < j \leq n+1$ denoting the last $n+2, \dots, m_q$ basis functions, and the nodal variables are defined by $N_i(v) = v(a_i)$ for $i = 1, \dots, n+1$, and

$$N_{ij}(v) = v(a_{ij}) - \frac{1}{2}(v(a_i) + v(a_j)) \quad \text{for } 1 \leq i < j \leq n+1.$$

1.3. **The finite element multigrid method.** We use the notation and framework presented in [7]. Let \mathcal{T}_1 be a triangulation and define \mathcal{T}_k for $k = 2, \dots, K$ recursively by subdividing all n -simplices in \mathcal{T}_{k-1} . Triangles are subdivided into four congruent sub-triangles connecting the edge midpoints as in Figure 1.1. Tetrahedra are subdivided into eight sub-tetrahedra by the regular refinement algorithm proposed in [5] and as depicted in Figure 1.2. We remark that the all sub-tetrahedra are not congruent but on repeating the process the sub-tetrahedra will remain shape-regular [5]. Hence the family of triangulations $\{\mathcal{T}_k\}_{k=1}^K$ will be quasi-uniform.

Set $h_1 = \max_{T \in \mathcal{T}_1} h_T$. It follows that $h_k = 2^{-k+1}h_1$ for $k = 1, \dots, K$, and for convenience we set $h = h_K$, and recall that the family $\{\mathcal{T}_k\}$ is *quasi-uniform* [9] if there is a constant $\beta > 0$ such that

$$(1.4) \quad \frac{h}{h_T} \leq \beta \quad \forall T \in \bigcup_k \mathcal{T}_k,$$

and if there is a constant $\gamma > 0$ such that

$$(1.5) \quad \frac{h_T}{\rho_T} \leq \gamma \quad \forall T \in \bigcup_k \mathcal{T}_k,$$

where $\rho_T = \sup\{\text{diam}(S) : S \text{ is a ball contained in } T\}$. A family of triangulations satisfying (1.5) is said to be *regular*.

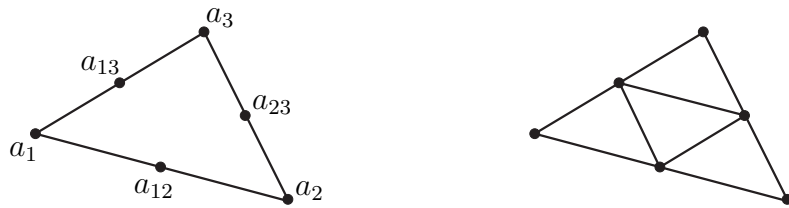


Figure 1.1: Regular triangle refinement. Original and refined triangles.

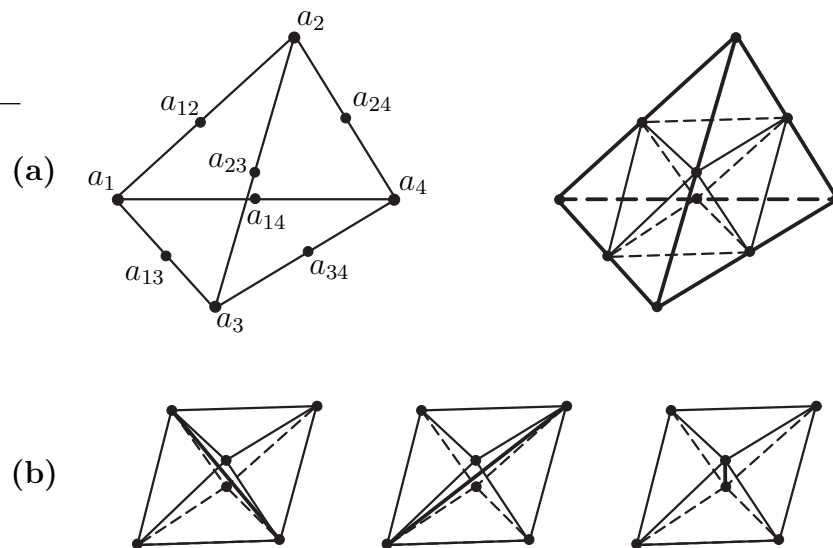


Figure 1.2: Regular tetrahedron refinement due to [5]. (a) Original and refined tetrahedron. (b) The interior octahedron is divided in one out of three ways as specified in [5].

In the usual way we define the piecewise continuous finite element spaces V_k on Ω by the finite elements $(T, \mathcal{P}_T, \mathcal{N}_T)_{T \in \mathcal{T}_k}$ with local basis functions $\{\varphi_{1,T}, \dots, \varphi_{m_q,T}\}$ and node variables $\mathcal{N}_T = \{N_{1,T}, N_{2,T}, \dots, N_{m_q,T}\}$.

Let $\{\phi_1, \dots, \phi_{M_k}\}$ be a basis for V_k with

$$(1.6) \quad \dim V_k := M_k = \text{card} \{L_q(T) : T \in \mathcal{T}_k\},$$

so that ϕ_i has support in S_i for $i = 1, \dots, M_k$ and where

$$(1.7) \quad S_i := \bigcup \{T \in \mathcal{T}_k : x_i \in T\},$$

for the *global nodes* $\{x_i\}_{i=1}^{M_k} = \{L_q(T) : T \in \mathcal{T}_k\}$.

For $T \in \mathcal{T}_k$ let I_T be an index set of the local nodes in the finite element $(T, \mathcal{P}_T, \mathcal{N}_T)$, for example, $I_T = \{1, 2, 3, 12, 13, 23\}$ for the quadratic Lagrange finite element in two dimensions. Let $i_j : I_T \rightarrow \{1, \dots, M_k\}$ be the injective map that maps the local index j to the corresponding global index i_j . We express the global basis functions in terms of the local finite element base functions. For $i = 1, \dots, M_k$ and with j so that $i_j = i$

$$(1.8) \quad \phi_i|_T = \begin{cases} \varphi_{j,T} & \text{if } T \in S_i, \\ 0 & \text{if } T \notin S_i. \end{cases}$$

Hence $V_k \ni v = \sum_{i=1}^{M_k} \tilde{v}_i \phi_i$, where $(\tilde{v}_1, \dots, \tilde{v}_{M_k}) = \tilde{v} \in \mathbf{R}^{M_k}$ is the coordinate vector with respect to the basis $\{\phi_1, \dots, \phi_{M_k}\}$.

Now $\{V_k\}_{k=1}^K$ is a nested sequence of finite element spaces, that is,

$$V_1 \subset V_2 \subset \dots \subset V_K \subset V.$$

From equation (1.1) we obtain the finite element equations on the K :th level

$$(1.9) \quad u \in V_K : \quad a(u, v) = (f, v) \quad \forall v \in V_K,$$

where we assume that $f \in V_K$ is a finite element approximation to the linear form $f(\cdot)$ in equation (1.1).

In order to describe the multigrid method we will need the following auxiliary operators. For $k = 1, \dots, K$ let $A_k : V_k \rightarrow V_k$ be defined by

$$(A_k v, \phi) = a(v, \phi) \quad \forall \phi \in V_k,$$

and the projectors $P_{k-1} : V_k \rightarrow V_{k-1}$ and $Q_{k-1} : V_k \rightarrow V_{k-1}$ defined by

$$a(P_{k-1} v, \phi) = a(v, \phi) \quad \forall \phi \in V_{k-1},$$

and

$$(Q_{k-1}v, \phi) = (v, \phi) \quad \forall \phi \in V_{k-1}.$$

We will also need a generic smoother $R_k : V_k \rightarrow V_k$ for $k = 1, \dots, K$ and denote by R_k^t the adjoint of R_k with respect to (\cdot, \cdot) .

By the coercivity of $a(\cdot, \cdot)$ and the inverse inequality we obtain lower and upper bounds to the eigenvalues of A_k ,

$$(1.10) \quad c_1 \|v\|_0^2 \leq (A_k v, v) = a(v, v) \leq c_2 h_k^{-2} \|v\|_0^2 \quad \forall v \in V_k,$$

that is, the largest eigenvalue λ_k of A_k is bounded by $c_2 h_k^{-2}$.

We consider the V-cycle multigrid algorithm. Given initial data $u^0 \in V_K$ the algorithm generates a sequence that approximates u , the solution to (1.9), by

$$(1.11) \quad u^{m+1} = \text{Mg}_K(u^m, f) \quad m = 0, 1, \dots,$$

where $\text{Mg}_K(\cdot, \cdot) : V_K \times V_K \rightarrow V_K$ is defined by the following algorithm [7].

Algorithm 1: $\text{Mg}_k(v, f)$

Input: multigrid level k , initial value $v = u^0$ as in (1.11) and right hand side f .

Output: u^1 in (1.11).

if $k = 1$ **then**

return $A_0^{-1} f$ /* exact solution */

else

$v' = v + R_\ell^t(f - A_k v)$ /* presmoothing */

$v'' = v' + \text{Mg}_{k-1}(0, Q_{k-1}(f - A_k v'))$ /* error correction */

return $v'' + R_k(f - A_k v'')$ /* postsmoothing */

If there exists $\omega > 0$ independent of K such that

$$(1.12) \quad \omega \lambda_k^{-1} \|v\|_0^2 \leq (\bar{R}_k v, v) \quad \forall v \in V_k, \quad k = 1, \dots, K,$$

where $\bar{R}_k = R_k + R_k^t - R_k^t A_k R_k$ is the symmetrized smoother, and if there is a constant C_P independent of K , such that

$$(1.13) \quad \|(I - P_{k-1})v\|_0^2 \leq C_P \lambda_k^{-1} (A_k v, v) \quad \forall v \in V_k, \quad k = 1, \dots, K,$$

then Algorithm 1 converges [6, 7] in the following way

$$(1.14) \quad \| \|u - u^m\| \| \leq \left(\frac{C_P}{C_P + \omega} \right)^m \| \|u - u^0\| \|.$$

We note that the convergence deteriorates when $\omega \downarrow 0$, and in order to achieve good convergence rates it will be fundamental to understand the properties of the smoother and try to make ω as large as possible. Below we will estimate ω for $n = 2, 3$, and $q = 1, 2$, and for different finite elements. This estimate qualitatively explains the poor performance of Algorithm 1 applied to finite element equations based on higher degree basis functions.

We now consider the case when R_k is the point Gauss-Seidel smoother. Decompose the space V_k into subspaces V_k^i spanned by the basis functions ϕ_i , for $i = 1, \dots, M_k$, that is,

$$(1.15) \quad V_k = V_k^1 \oplus \dots \oplus V_k^{M_k}.$$

Let κ be the interaction matrix reflecting the coupling between the subspaces V_k^i and defined by

$$\kappa_{ij} = \begin{cases} 0 & \text{if } (A_k v_i, v_j) = 0, \\ 1 & \text{otherwise,} \end{cases} \quad \text{for } v_i \in V_k^i \text{ and } v_j \in V_k^j.$$

If there is a positive number C_1 , independent of k , such that

$$(1.16) \quad \|\kappa\|_2 \leq \|\kappa\|_\infty \leq C_1,$$

where $\|\cdot\|$ denotes the appropriate matrix norm, and if there is a positive constant C_2 , independent of k , such that

$$(1.17) \quad \sum_{i=1}^{M_k} \|v_i\|_0^2 \leq C_2 \|v\|_0^2 \quad \text{for } v \in V_k \text{ and } v_i \in V_k^i,$$

then (1.12) holds with

$$(1.18) \quad \omega = (C_2 C_1^2)^{-1},$$

see [7, Theorem 82, p. 277] for a more general statement.

1.3.1. *Estimating C_1 .* We note that C_1 is the maximal number of indices j such that $(A_k v_i, v_j) \neq 0$ for $i, j = 1, \dots, M_q$. It is bounded by

$$(1.19) \quad C_1 \leq \max_{1 \leq i \leq M_k} \text{card} \{L_q(T) : T \in S_i\},$$

where we used the notation in (1.6) and (1.7). The number of global nodes in S_i and hence C_1 will differ quite significantly as n and q varies, see Figure 1.3.

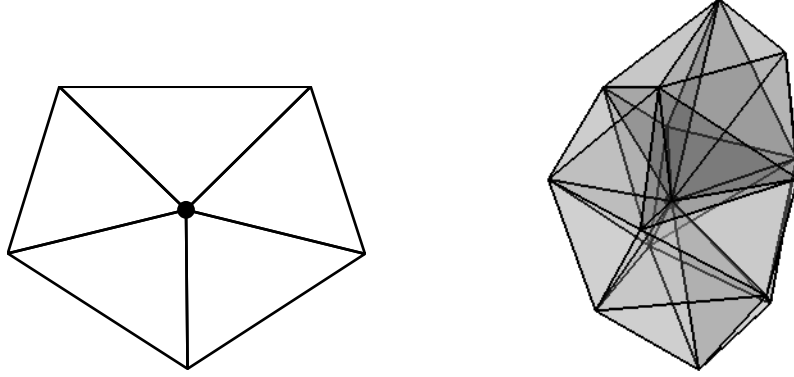


Figure 1.3: Examples of S_i from the triangulations depicted in Figure 2.1. **(left)** For $n = 2$ there are 5 triangles, 6 nodes and 10 edges. **(right)** For $n = 3$ there are 24 tetrahedra, 15 nodes and 50 edges.

1.3.2. *Estimating C_2 .* Since V_k is finite dimensional the norms $\|v\|_0$ and $\|\tilde{v}\|$ are equivalent in V_k . In other words we have the following estimates

$$(1.20) \quad \alpha_1 \|v\|_0^2 \leq ch_k^n \|\tilde{v}\|^2 \leq \alpha_2 \|v\|_0^2 \quad \forall v \in V_k,$$

for some constants c , α_1 and α_2 that we will estimate below in the case the family of triangulations $\{\mathcal{T}_k\}_{k=1}^K$ is quasi-uniform. With (1.20) we readily verify (1.17) since

$$\sum_{i=1}^{M_k} \|v_i\|_0^2 \leq ch_k^n \alpha_1^{-1} \sum_{i=1}^{M_k} \tilde{v}_i^2 \leq \frac{\alpha_2}{\alpha_1} \|v\|_0^2,$$

and thus $C_2 = \alpha_2/\alpha_1$.

In order to derive (1.20) we first derive a similar, but local, estimate. For any $T \in \mathcal{T}_k$ we have $v|_T = \sum_{j=1}^{m_q} \tilde{v}_{i_j} \varphi_{j,T}$ and since all finite elements on $T \in \mathcal{T}_k$ are affine equivalent to the reference finite elements we get, by a change of variables,

$$(1.21) \quad \|v\|_{0,T}^2 = (v, v)_T = |\det B^{-1}| \sum_{j,\ell=1}^{m_q} (\tilde{v}_{i_j} \hat{\varphi}_{j,T}, \tilde{v}_{i_\ell} \hat{\varphi}_{\ell,T})_{\hat{T}},$$

where $|\det B^{-1}| = |\widehat{T}|/|T|$ and with B as in (1.3).

Let $\underline{\mu}$ and $\bar{\mu}$ denote the smallest and largest eigenvalues to the symmetric and positive definite matrix

$$(1.22) \quad [\mathcal{M}_{\widehat{T}}]_{j\ell} = |\widehat{T}|(\hat{\varphi}_{j,\widehat{T}}, \hat{\varphi}_{\ell,\widehat{T}})_{\widehat{T}} \quad \text{for } j, \ell = 1, \dots, m_q,$$

and estimate (1.21)

$$|T|\underline{\mu} \sum_{j=1}^{m_q} \tilde{v}_{i_j}^2 \leq \sum_{j,\ell=1}^{m_q} (\tilde{v}_{i_j} \hat{\varphi}_{j,\widehat{T}}, \tilde{v}_{i_\ell} \hat{\varphi}_{\ell,\widehat{T}})_{\widehat{T}} \leq |T|\bar{\mu} \sum_{j=1}^{m_q} \tilde{v}_{i_j}^2 \quad \forall \tilde{v}_{i_j} \in \mathbf{R}.$$

Since the triangulation is quasi-uniform

$$\frac{h_k}{\beta\gamma} \leq \frac{h_T}{\gamma} \leq \rho_T \leq c^{-1/n}|T|^{1/n} \quad \text{and} \quad c^{-1/n}|T|^{1/n} \leq h_T \leq h_k,$$

where $c^n = \pi/(2n)$, we get

$$(\beta\gamma)^{-n} \underline{\mu} \sum_{j=1}^{m_q} \tilde{v}_{i_j}^2 \leq \sum_{j,\ell=1}^{m_q} ch_k^{-n} (\tilde{v}_{i_j} \varphi_{j,T}, \tilde{v}_{i_\ell} \varphi_{\ell,T})_T \leq \bar{\mu} \sum_{j=1}^{m_q} \tilde{v}_{i_j}^2 \quad \forall \tilde{v}_{i_j} \in \mathbf{R}$$

Let $\sigma_i = \text{card}(S_i)$, that is, σ_i is the number of n -simplices the global node x_i intersect, and set

$$\underline{\sigma} = \min_{1 \leq i \leq M_k} \sigma_i \quad \text{and} \quad \bar{\sigma} = \max_{1 \leq i \leq M_k} \sigma_i.$$

Now (1.20) follows from the local estimate above by summing over all $T \in \mathcal{T}_k$ and taking into account that one node x_i could appear in several n -simplices which is reflected in the parameter σ_i . Thus

$$(\beta\gamma)^{-n} \underline{\sigma} \underline{\mu} \|\tilde{v}\|^2 \leq ch_k^{-n} \|v\|_0^2 \leq \bar{\sigma} \bar{\mu} \|\tilde{v}\|^2,$$

or

$$(\bar{\sigma} \bar{\mu})^{-1} \|v\|_0^2 \leq ch_k^n \|\tilde{v}\|^2 \leq (\beta\gamma)^n (\underline{\sigma} \underline{\mu})^{-1} \|v\|_0^2 \quad \forall v \in V_k,$$

where we now identify the constants in (1.20)

$$\alpha_1 = (\bar{\sigma} \bar{\mu})^{-1} \quad \text{and} \quad \alpha_2 = (\beta\gamma)^n (\underline{\sigma} \underline{\mu})^{-1},$$

and hence

$$(1.23) \quad C_2 = (\beta\gamma)^n \frac{\bar{\sigma} \bar{\mu}}{\underline{\sigma} \underline{\mu}}.$$

We note the relatively strong dependence of C_2 on β and γ . This implies that the point Gauss-Seidel smoother will deteriorate: (1) if the family of

triangulations $\{\mathcal{T}_k\}_{k=1}^K$ is not quasi-uniform, β increases with k , for example, when \mathcal{T}_k is adaptively refined, or (2) if the $\{\mathcal{T}_k\}_{k=1}^K$ is not regular, γ increases with k , for example, if the refinement algorithm does not preserve the shape-regularity (1.5).

2. NUMERICAL EXPERIMENTS

In matrix form (1.9) becomes

$$\mathcal{A}\tilde{u} = \mathcal{F},$$

where \mathcal{A} denote the matrix $[\mathcal{A}]_{ij} = (A_K\phi_i, \phi_j)$ for $i = 1, \dots, M_q$ and $\tilde{u} \in \mathbf{R}^{M_q}$ denote the coordinate vector with respect to the finite element basis and $\mathcal{F} = (\mathcal{F}_1, \dots, \mathcal{F}_{M_q})$ where $\mathcal{F}_i = (f, \phi_i)$. We solve this linear system using the V-cycle Algorithm 1 with $\tilde{u}^0 = 0$ and iterate $m = 1, 2, \dots$ until the relative residual

$$\text{Res} := \frac{\|\mathcal{F} - \mathcal{A}\tilde{u}^m\|}{\|\mathcal{F}\|}$$

is less than a specified tolerance 'Tol'. In this work we use the Tol = 10^{-6} . Note that the relative tolerance times a constant is always greater than $\|u - u^m\|_{1,\Omega}$ where u is the finite element solution we are approximating, cf. [11, Proposition 9.19, p. 393].

By the *work* we mean the number of arithmetic operations required for Algorithm 1 to converge or equally we measure the 'Time' for the algorithm to converge.

In order to examine the optimality of the algorithm we measure the 'Time' for different number of degrees of freedom, 'Dof', and solve the least square problem

$$\text{Time} = a(\text{Dof})^b$$

for the parameters a, b .

Below we exhibit three different numerical experiments that will elucidate the theory outline in the sections above. We use the point Gauss-Seidel smoother in all experiments and we vary $n = 2, 3$ and $q = 1, 2$ for the Lagrange finite element. For $q = 2$ also we compare with the hierarchical finite element in Section 1.2.2.

The experiments are:

- In the first experiment we consider triangulations of the n -unit cube in Figure 2.1 and estimate ω appearing in the convergence estimate (1.14).

- In the second experiment we solve the Poisson equation using the V-cycle multigrid Algorithm 1 and examine the optimality in case of problems with: (1) full regularity and (2) less than full regularity.
- In the third experiment we use the multigrid solver to precondition a Stokes solver and examine the optimality of the Stokes solver for problems with less than full regularity.

2.1. **Estimating w for the point Gauss-Seidel smoother.** In order to indicate how ω in (1.14) varies as a function of $n = 2, 3$ and $q = 1, 2$ and the type of finite element, Lagrange or hierarchical, we estimate C_1 and C_2 for triangulations of the n -unit cube in Figure 2.1 and compute ω from (1.18).

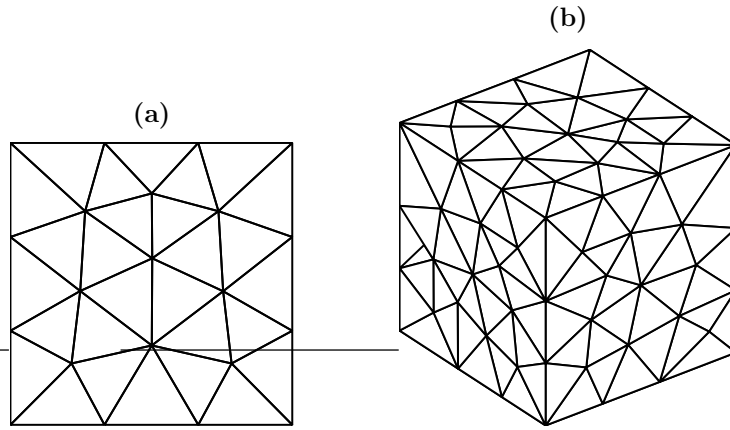


Figure 2.1: Triangulations \mathcal{T}_0 of the n -unit cube. (a) $n = 2$. (b) $n = 3$.

We summarize the results in Table 2.1 and give account for the estimates of C_1 and C_2 in the subsequent sections.

2.1.1. *Estimating C_1 .* We estimate C_1 by (1.19) for the triangulations in Figure 2.1. When $q = 1$ we count the number of vertices and when $q = 2$ we count the number of vertices and edges for every S_i . We summarize the results in Table 2.2.

2.1.2. *Estimating C_2 .* We estimate C_2 by (1.23) for the triangulations in Figure 2.1. The parameter in (1.23) are computed and the data is gathered in Tables 2.3 and 2.4 and finally we obtain C_2 in Table 2.5.

Table 2.1: ω in (1.14) computed for the triangulations in Figure 2.1. h denote hierarchical finite elements and the remaining data are for Lagrange finite elements.

(n, q)	(2, 1)	(2, 2)	(2, 2h)	(3, 1)	(3, 2)	(3, 2h)
ω^{-1}	$1.0 \cdot 10^4$	$3.3 \cdot 10^5$	$1.1 \cdot 10^6$	$9.0 \cdot 10^7$	$1.3 \cdot 10^{10}$	$4.6 \cdot 10^{10}$

Table 2.2: The maximum number of n -simplices, vertices and edges in S_i for $i = 1, \dots, M_q$ with respect to i and C_1 for the triangulations in Figure 2.1.

max no. of:	n -simplices	vertices	edges	vertices+edges
$n = 2$	8	8	14	22
$n = 3$	40	23	82	105
$(n, q):$	(2,1)	(2,2)	(3,1)	(3,2)
C_1	8	22	23	105

Table 2.3: Parameters in (1.23) only depending on n and for the triangulations in Figure 2.1.

	β	γ	$\underline{\sigma}$	$\bar{\sigma}$
$n = 2$	2.0	1.6	2	8
$n = 3$	4.3	3.5	4	40

3. THE POISSON EQUATION

We consider the following Poisson equation with mixed Dirichlet-Neumann boundary conditions on bounded polyhedral domains $\Omega \subset \mathbf{R}^n$ for $n = 2, 3$,

$$-\Delta u = f \quad \text{in } \Omega, \quad u = g \quad \text{on } \partial\Omega_D, \quad \text{and } \nu \cdot \nabla u = 0 \quad \text{on } \partial\Omega_N,$$

where the boundary is partitioned so that $\partial\Omega_D \cup \partial\Omega_N = \partial\Omega$, g is a constant, ν is the outward normal to the boundary and we assume $f \in H^{-1}(\Omega)$ and

Table 2.4: Parameters in (1.23) and for the triangulations in Figure 2.1. h denote hierarchical finite elements and the remaining data are for Lagrange finite elements.

(n, q)	(2, 1)	(2, 2)	(2, 2h)	(3, 1)	(3, 2)	(3, 2h)
$\underline{\mu}$	0.083	0.021	0.011	0.050	0.007	0.004
$\bar{\mu}$	0.333	0.357	0.678	0.250	0.261	0.494
$\bar{\mu}/\underline{\mu}$	4	17	62	5	36	128

Table 2.5: C_2 for the triangulations in Figure 2.1. h denote hierarchical finite elements and the remaining data are for Lagrange finite elements.

(n, q)	(2, 1)	(2, 2)	(2, 2h)	(3, 1)	(3, 2)	(3, 2h)
C_2	164	696	$2.5 \cdot 10^3$	$1.7 \cdot 10^5$	$1.2 \cdot 10^6$	$4.2 \cdot 10^6$

thus the problem is a well posed. Let

$$V = \{u \in H^1(\Omega) : u = 0 \text{ on } \partial\Omega_D\}.$$

Now the bilinear and linear forms in Section 1.1 are

$$a(u, v) = \int_{\Omega} \nabla u \cdot \nabla v \, dx,$$

and

$$f(v) = \int_{\Omega} f v \, dx.$$

With $u_g \in H^1(\Omega)$ denoting the extension of g , the weak formulation to the above Poisson problem follows as usual and reads, find $u \in H^1(\Omega)$ such that

$$(3.1) \quad \begin{aligned} u &= u_g + \phi, & \phi &\in V, \\ a(\phi, v) &= f(v) - a(u_g, v) & \forall v &\in V. \end{aligned}$$

3.0.3. *Model problem I —full regularity.* In this case we let $\Omega = [0, 1]^n$ be the n -unit cube depicted in Figure 2.1. Set $f = n\pi^2 \prod_{i=1}^n \sin(\pi x_i)$, $g = 0$ and $\partial\Omega_N = \emptyset$. Since Ω is convex the solution $u \in H^2(\Omega) \cap H_0^1(\Omega)$, that is

full regularity. We note that (1.13) will be satisfied also for higher degree finite elements which could be inferred from the usual duality argument.

Let $w \in H^2(\Omega) \cap H_0^1(\Omega)$ be the solution to the dual problem

$$w \in H_0^1(\Omega) \quad a(w, \phi) = (g, \phi) \quad \forall \phi \in H_0^1(\Omega),$$

where w satisfies the regularity estimate

$$\|w\|_2 \leq C\|g\|_0,$$

and where we have the error estimate

$$\|(I - P_{k-1})w\|_1 \leq Ch_{k-1}\|w\|_2$$

Thus, for $v \in H^2(\Omega) \cap H_0^1(\Omega)$ and taking $g = (I - P_{k-1})v$ and $\phi = (I - P_{k-1})v$ and due to the Galerkin orthogonality and with the above estimates

$$\begin{aligned} \|(I - P_{k-1})v\|_0^2 &= a(w, (I - P_{k-1})v) \\ &= a((I - P_{k-1})w, (I - P_{k-1})v) \\ &\leq C\|(I - P_{k-1})w\|_1\|(I - P_{k-1})v\|_1 \\ &\leq Ch_{k-1}\|w\|_2\|(I - P_{k-1})v\|_1 \\ &\leq Ch_{k-1}\|(I - P_{k-1})v\|_0\|v\|_1 \end{aligned}$$

and (1.13) follows since $h_{k-1} \leq C\lambda_{k-1}^{-1/2}$ which follows from (1.10).

We solve the problem for different finite element approximations with the V-cycle multigrid Algorithm 1 and for $K = 6$, $n = 2$ and $K = 3$, $n = 3$. The results from these experiments are summarized in Figure 3.1 and Tables 3.1 and 3.2.

3.0.4. Model problem II —less than full regularity. In this case we let Ω be the L-shaped domain with one reentrant edge, $\Omega = \{(x, y) \in [0, 2]^2 \setminus [1, 2] \times [0, 1]\}$ for $n = 2$ and $\Omega = \{(x, y, z) \in [0, 2]^2 \times [0, 0.5] \setminus [1, 2] \times [0, 1] \times [0, 0.5]\}$ for $n = 3$, see Figure 3.2. Let $\partial\Omega_D = \partial\Omega_{D_0} \cup \partial\Omega_{D_1}$ where $\partial\Omega_{D_0} = \{(x, y) : x = 1, y \in [1, 2]\}$ and $\partial\Omega_{D_1} = \{(x, y) : x \in [0, 1], y = 0\}$ for $n = 2$ and $\partial\Omega_{D_0} = \{(x, y, z) : x = 2, (y, z) \in [1, 2] \times [0, 0.5]\}$ and $\partial\Omega_{D_1} = \{(x, y, z) : (x, z) \in [0, 1] \times [0, 0.5], y = 0\}$ for $n = 3$. Set $f = 0$, $g = 0$ on $\partial\Omega_{D_0}$ and $g = 1$ on $\partial\Omega_{D_1}$. Since Ω is non-convex we $u \in H^{1+\alpha}(\Omega) \cap H_0^1(\Omega)$ for $0 < \alpha \leq 1$, that is, less than full regularity. The analysis above will not immediately apply, however it is possible to generalize the analysis to include this case [7].

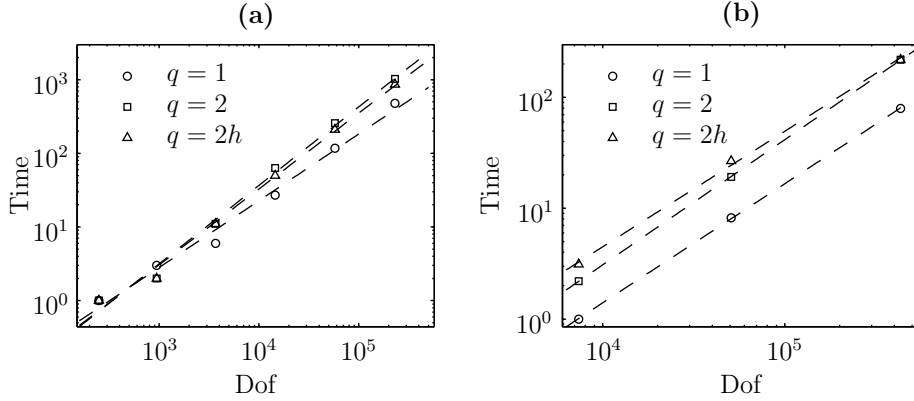


Figure 3.1: Convergence time 'Time' for the V-cycle multigrid Algorithm 1 as a function of 'Dof' and for different finite elements and the triangulations in Figure 2.1. h denote hierarchical finite elements and the remaining data are for Lagrange finite elements (a) $n = 2$ (b) $n = 3$.

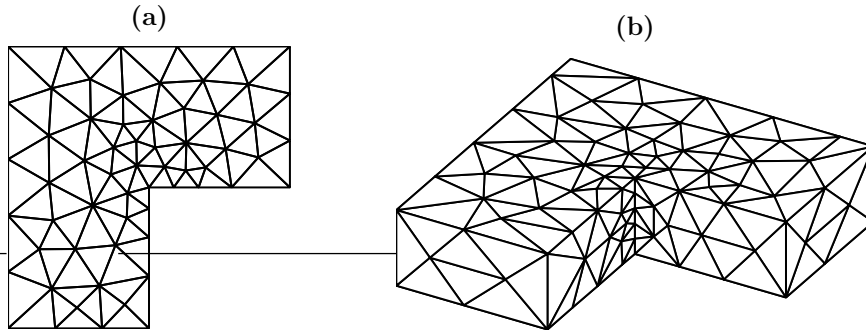


Figure 3.2: Triangulations \mathcal{T}_0 of the L-shaped domain. (a) $n = 2$. (b) $n = 3$

We solve the problem for different finite element approximations with the V-cycle multigrid Algorithm 1 and for $K = 6$, $n = 2$ and $K = 3$, $n = 3$. The results from these experiments are summarized in Figure 3.3 and Tables 3.1 and 3.2.

3.1. Stokes equations with less than full regularity. Let Ω be a the polyhedral domains illustrated in Figures 3.4 and 3.5 which we refer to as the Ridge Domain and the Herringbone Domain, respectively. Consider

Table 3.1: Convergence data for the V-cycle multigrid algorithm 1 applied to Model Problem I and II for $n = 2$ and the finite elements in Section 1.2.

Model problem I, $(n, q) = (2, 1)$ $a = 5.4 \cdot 10^{-3}, b = 0.91$				Model problem I, $(n, q) = (2, 2)$ $a = 2.0 \cdot 10^{-3}, b = 1.07$			
k	Dof	m	Res	k	Dof	m	Res
1	249	4	$3.3 \cdot 10^{-8}$	1	249	4	$2.1 \cdot 10^{-7}$
2	945	4	$1.0 \cdot 10^{-7}$	2	945	4	$6.6 \cdot 10^{-7}$
3	3681	4	$1.6 \cdot 10^{-7}$	3	3681	4	$9.3 \cdot 10^{-7}$
4	14529	4	$2.2 \cdot 10^{-7}$	4	14529	5	$4.6 \cdot 10^{-8}$
5	57729	4	$2.5 \cdot 10^{-7}$	5	57729	5	$5.0 \cdot 10^{-8}$
6	230145	4	$2.8 \cdot 10^{-7}$	6	230145	5	$5.2 \cdot 10^{-8}$

Model problem I, $(n, q) = (2, 2h)$ $a = 2.5 \cdot 10^{-3}, b = 1.03$				Model problem II, $(n, q) = (2, 1)$ $a = 2.5 \cdot 10^{-3}, b = 1.03$			
k	Dof	m	Res	k	Dof	m	Res
1	249	4	$8.0 \cdot 10^{-8}$	1	817	4	$1.4 \cdot 10^{-8}$
2	945	4	$2.3 \cdot 10^{-7}$	2	3169	4	$1.1 \cdot 10^{-7}$
3	3681	4	$3.0 \cdot 10^{-7}$	3	12481	4	$4.0 \cdot 10^{-7}$
4	14529	4	$3.3 \cdot 10^{-7}$	4	49534	4	$9.5 \cdot 10^{-7}$
5	57729	4	$3.4 \cdot 10^{-7}$	5	197377	5	$4.6 \cdot 10^{-8}$
6	230145	4	$4.4 \cdot 10^{-7}$	6	787969	5	$8.5 \cdot 10^{-8}$

Model problem II, $(n, q) = (2, 2)$ $a = 3.0 \cdot 10^{-3}, b = 0.99$				Model problem II, $(n, q) = (2, 2h)$ $a = 1.2 \cdot 10^{-3}, b = 1.06$			
k	Dof	m	Res	k	Dof	m	Res
1	817	4	$3.1 \cdot 10^{-7}$	1	817	4	$4.4 \cdot 10^{-7}$
2	3669	5	$4.8 \cdot 10^{-8}$	2	3169	5	$2.8 \cdot 10^{-8}$
3	12481	5	$1.3 \cdot 10^{-7}$	3	12481	5	$4.0 \cdot 10^{-8}$
4	49534	5	$2.5 \cdot 10^{-7}$	4	49534	5	$5.7 \cdot 10^{-8}$
5	197377	5	$4.3 \cdot 10^{-7}$	5	197377	5	$7.8 \cdot 10^{-8}$
6	787969	5	$6.6 \cdot 10^{-7}$	6	787969	5	$1.1 \cdot 10^{-7}$

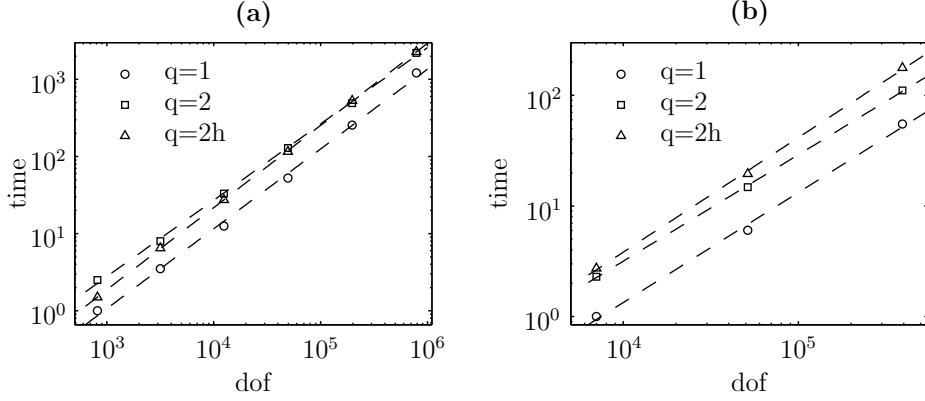


Figure 3.3: Convergence time 'Time' for the V-cycle multigrid Algorithm 1 as a function of 'Dof' and for different finite elements and the triangulations in Figure 3.2. h denote hierarchical finite elements and the remaining data are for Lagrange finite elements (a) $n = 2$ (b) $n = 3$.

the periodic Stokes problem in dimensionless form

$$\begin{aligned}
 (3.2) \quad & -\Delta u + \nabla p = 0 \quad \text{in } \Omega, \\
 & \nabla \cdot u = 0 \quad \text{in } \Omega, \\
 & u = 0 \quad \text{on } \partial\Omega \setminus (\Gamma_A \cup \Gamma_B), \\
 & u|_{\Gamma_A} = u|_{\Gamma_B}, \\
 & p|_{\Gamma_A} = p|_{\Gamma_B} + R,
 \end{aligned}$$

where u is the unknown velocity field, p is the unknown pressure and R is a constant modelling the pressure drop. We note that this model is inspired by [22] where fluid mixing in micro channels was studied experimentally.

Let

$$V = \{u \in H^1(\Omega)^3 : u = 0 \text{ on } \partial\Omega \setminus (\Gamma_A \cup \Gamma_B) \text{ and } u|_{\Gamma_A} = u|_{\Gamma_B}\}.$$

and $W = L^2(\Omega)/\mathbf{R}$.

Then following the standard procedure, see for example [12, 18], we obtain the weak formulation. Find $(u, p) \in V \times W$ such that

$$(3.3) \quad a(u, \phi) + b(\phi, p) - b(u, \lambda) = Rl(v) \quad \forall (\phi, \lambda) \in V \times W,$$

Table 3.2: Convergence data for the V-cycle multigrid algorithm 1 applied to Model Problem I and II for $n = 3$ and the finite elements in Section 1.2.

Model problem I, $(n, q) = (3, 1)$ $a = 7.1 \cdot 10^{-5}, b = 1.07$				Model problem I, $(n, q) = (3, 2)$ $a = 9.4 \cdot 10^{-5}, b = 1.13$			
k	Dof	m	Res	k	Dof	m	Res
1	7377	4	$2.1 \cdot 10^{-7}$	1	7377	4	$5.0 \cdot 10^{-8}$
2	50713	5	$2.1 \cdot 10^{-7}$	2	50713	5	$2.1 \cdot 10^{-7}$
3	432961	6	$7.8 \cdot 10^{-7}$	3	432961	7	$3.6 \cdot 10^{-7}$

Model problem I, $(n, q) = (3, 2h)$ $a = 3.0 \cdot 10^{-4}, b = 1.04$				Model problem II, $(n, q) = (3, 1)$ $a = 1.4 \cdot 10^{-4}, b = 1.0$			
k	Dof	m	Res	k	Dof	m	Res
1	7377	6	$4.5 \cdot 10^{-7}$	1	7005	4	$1.2 \cdot 10^{-7}$
2	50713	6	$9.3 \cdot 10^{-7}$	2	50713	5	$9.6 \cdot 10^{-8}$
3	432961	7	$8.7 \cdot 10^{-7}$	3	393617	6	$1.3 \cdot 10^{-7}$

Model problem II, $(n, q) = (3, 2)$ $a = 4.5 \cdot 10^{-4}, b = 0.96$				Model problem II, $(n, q) = (3, 2h)$ $a = 2.8 \cdot 10^{-4}, b = 1.04$			
k	Dof	m	Res	k	Dof	m	Res
1	7005	4	$1.9 \cdot 10^{-7}$	1	7005	6	$5.0 \cdot 10^{-7}$
2	51433	5	$8.0 \cdot 10^{-8}$	2	51433	7	$2.9 \cdot 10^{-7}$
3	393617	5	$4.4 \cdot 10^{-7}$	3	393617	7	$2.6 \cdot 10^{-7}$

where

$$a(u, \phi) = \int_{\Omega} \sum_{i,j=1}^n \frac{\partial u_i}{\partial x_j} \frac{\partial \phi_i}{\partial x_j} dx,$$

$$b(\phi, p) = - \int_{\Omega} (\nabla \cdot \phi) p dx,$$

$$l(v) = \int_{\Gamma_A} v \cdot \nu dS.$$

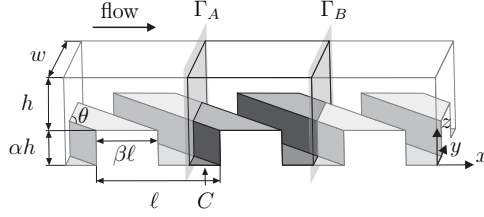


Figure 3.4: Three juxtaposed Ridge Domains. The shaded planes Γ_A and Γ_B are periodic boundaries. We choose the following values for the parameters: $\ell = w = 1$, $h = 0.3$, $\theta = 45^\circ$, $\alpha = 2/3$, $\beta = 0.5$, and the length of the unit cell is $= 1$.

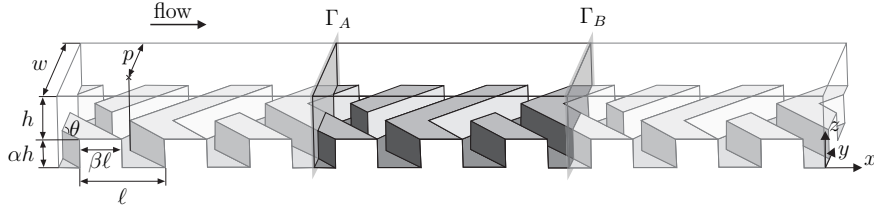


Figure 3.5: Three juxtaposed Herringbone Domains. The shaded planes Γ_A and Γ_B are periodic boundaries. We choose the following values for the parameters: $\ell = 2/3$, $w = 1$, $h = 1/5$, $\theta = 45^\circ$, $\alpha = 2/3$, $\beta = 9/16$, $p = 2/3$, and the length of the unit cell is $= 14/9$.

We discretize (3.3) using the P_2P_1 Taylor-Hood finite elements and obtain the saddle point problem

$$(3.4) \quad \begin{pmatrix} A & B^T \\ B & 0 \end{pmatrix} \begin{pmatrix} u_h \\ p_h \end{pmatrix} = \begin{pmatrix} l_h \\ 0 \end{pmatrix},$$

for matrices A , B and where T denotes the transpose. There are many plausible way to solve this problem approximately, by some iterative scheme, see the survey paper [4]. In this work we use the method proposed in [10, 17], for solving the stationary Navier-Stokes equations. The method is optimal and is based on the observation that the matrix

$$\begin{pmatrix} A & B^T \\ 0 & BA^{-1}B^T \end{pmatrix}^{-1} \begin{pmatrix} A & B^T \\ B & 0 \end{pmatrix}$$

has at most three eigenvalues [19, 15]. Thus, a Krylov method applied to the preconditioned system will converge to the exact solution in less than four iterations.

In practice the matrix in the (2,2) position of the preconditioning block matrix, $BA^{-1}B^T$ (the Schur complement), is not readily inverted but since $BA^{-1}B^T$ is spectrally equivalent to the pressure mass matrix (or Gram matrix) M_p we substitute $BA^{-1}B^T$ by M_p . Hence we precondition (3.4) with

$$\begin{pmatrix} A & B^T \\ 0 & M_p \end{pmatrix}^{-1},$$

and consequently a Krylov solver will now converge in a relatively small number of iterates almost independent of the size of the problem. The method is optimal.

In this work we use a flexible GMRES algorithm [20] to solve (3.4). In the preconditioning we approximate A^{-1} by two cycles of the V-cycle Algorithm 1 with five point Gauss-Seidle smoothing iterations on each level and M_p^{-1} is approximated by a few iterations with the flexible GMRES method preconditioned by five iterations of the point Gauss-Seidle solver. We note that since the saddle point problem is symmetric we could have used a MINRES Krylov solver instead.

In Table 3.3 we summarize the data from the experiments and note that the solver is almost optimal.

Table 3.3: Convergence data for the Stokes solver with V-cycle multigrid preconditioning.

Ridge Domain				Herringbone Domain			
levels	dof	m	Res	levels	dof	m	res
0	23654	24	$6.4 \cdot 10^{-7}$	0	32999	33	$8.6 \cdot 10^{-7}$
1	166599	27	$7.8 \cdot 10^{-7}$	1	232448	37	$8.6 \cdot 10^{-7}$
2	1245487	27	$1.0 \cdot 10^{-6}$	2	1736817	39	$8.4 \cdot 10^{-7}$
3	9621069	28	$9.6 \cdot 10^{-7}$				

4. DISCUSSION

We have demonstrated that the finite element multigrid method in practice works well for quadratic finite elements. Comparing the method applied to quadratic Lagrange finite element and the quadratic hierarchical finite element showed a convergence in favor of the Lagrange approximation. The estimates of ω seem to be overestimates. However, the estimates are probably qualitatively correct.

APPENDIX A. EIGENVALUES TO $\mathcal{M}_{\hat{T}}$

We give account for the calculation of the eigenvalues to the matrix

$$\mathcal{M}_{\hat{T}} = (\hat{\varphi}_{j,\hat{T}}, \hat{\varphi}_{\ell,\hat{T}})_{\hat{T}} \quad \text{for } j, \ell = 1, \dots, m_q,$$

for $n = 2, 3$ and Lagrange finite elements of degree $q = 1, 2$ and for $q = 2$ and the hierarchical base functions in Section 1.2.2. Note that we have omitted the factor $|\hat{T}| = 1/(2(n-1))$ in (1.22) since in the end we are interested in the ratio $\bar{\mu}/\underline{\mu}$ of the largest to smallest eigenvalues.

We recall and use the following relation [9, eq. (25.14), p. 187]

$$\int_T \lambda_{1,T}^{m_1} \lambda_{2,T}^{m_2} \cdots \lambda_{n+1,T}^{m_{n+1}} dx = |T| \frac{m_1! m_2! \cdots m_{n+1}! n!}{(m_1 + m_2 + \cdots + m_{n+1} + n)!}$$

where m_j are positive integers.

q = 1 and n = 2 Lagrange.

$$\mathcal{M}_T = 1/12 \begin{pmatrix} 2 & 1 & 1 \\ 1 & 2 & 1 \\ 1 & 1 & 2 \end{pmatrix},$$

with $\underline{\mu} = 1/24$ and $\bar{\mu} = 1/6$, $\bar{\mu}/\underline{\mu} = 4$.

q = 1 and n = 3 Lagrange.

$$\mathcal{M}_T = 1/20 \begin{pmatrix} 2 & 1 & 1 & 1 \\ 1 & 2 & 1 & 1 \\ 1 & 1 & 2 & 1 \\ 1 & 1 & 1 & 2 \end{pmatrix},$$

with $\underline{\mu} = 1/12$ and $\bar{\mu} = 1/4$, $\bar{\mu}/\underline{\mu} = 5$.

q = 2 and n = 2 Lagrange.

$$\mathcal{M}_T = 1/180 \begin{pmatrix} 6 & -1 & -1 & 0 & -4 & 0 \\ -1 & 6 & -1 & 0 & 0 & -4 \\ -1 & -1 & 6 & -4 & 0 & 0 \\ 0 & 0 & -4 & 32 & 16 & 16 \\ -4 & 0 & 0 & 16 & 32 & 16 \\ 0 & -4 & 0 & 16 & 16 & 32 \end{pmatrix},$$

with $\underline{\mu} = (17 - \sqrt{229})/90 \approx 0.021$ and $\bar{\mu} = (17 + \sqrt{229})/90 \approx 0.357$,
 $\bar{\mu}/\underline{\mu} \approx 17$.

q = 2h and n = 2 hierarchical.

$$\mathcal{M}_T = 1/180 \begin{pmatrix} 0 & 30 & 30 & 48 & 24 & 48 \\ 30 & 60 & 30 & 48 & 48 & 24 \\ 30 & 30 & 60 & 24 & 48 & 48 \\ 48 & 48 & 24 & 64 & 32 & 32 \\ 24 & 48 & 48 & 32 & 64 & 32 \\ 48 & 24 & 48 & 32 & 32 & 64 \end{pmatrix},$$

with $\underline{\mu} = (31 - \sqrt{901})/90 \approx 0.011$ and $\bar{\mu} = (31 + \sqrt{901})/90 \approx 0.678$,
 $\bar{\mu}/\underline{\mu} \approx 62$.

q = 2 and n = 3 Lagrange.

$$\mathcal{M}_T = 1/420 \begin{pmatrix} 6 & 1 & 1 & 1 & -4 & -6 & -4 & -4 & -6 & -6 \\ 1 & 6 & 1 & 1 & -4 & -4 & -6 & -6 & -4 & -6 \\ 1 & 1 & 6 & 1 & -6 & -4 & -4 & -6 & -6 & -4 \\ 1 & 1 & 1 & 6 & -6 & -6 & -6 & -4 & -4 & -4 \\ -4 & -4 & -6 & -6 & 32 & 16 & 16 & 16 & 16 & 8 \\ -6 & -4 & -4 & -6 & 16 & 32 & 16 & 8 & 16 & 16 \\ -4 & -6 & -4 & -6 & 16 & 16 & 32 & 16 & 8 & 16 \\ -4 & -6 & -6 & -4 & 16 & 8 & 16 & 32 & 16 & 16 \\ -6 & -4 & -6 & -4 & 16 & 16 & 8 & 16 & 32 & 16 \\ -6 & -6 & -4 & -4 & 8 & 16 & 16 & 16 & 16 & 32 \end{pmatrix},$$

with $\underline{\mu} = (113 - 5\sqrt{457})/840 \approx 0.007$ and $\bar{\mu} = (113 + 5\sqrt{457})/840 \approx 0.261$,
 $\bar{\mu}/\underline{\mu} \approx 36$.

$\mathbf{q} = 2\mathbf{h}$ and $\mathbf{n} = 3$ hierarchical.

$$\mathcal{M}_T = 1/420 \begin{pmatrix} 42 & 21 & 21 & 21 & 28 & 14 & 28 & 28 & 14 & 14 \\ 21 & 42 & 21 & 21 & 28 & 28 & 14 & 14 & 28 & 14 \\ 21 & 21 & 42 & 21 & 14 & 28 & 28 & 14 & 14 & 28 \\ 21 & 21 & 21 & 42 & 14 & 14 & 14 & 28 & 28 & 28 \\ 28 & 28 & 14 & 14 & 32 & 16 & 16 & 16 & 16 & 8 \\ 14 & 28 & 28 & 14 & 16 & 32 & 16 & 8 & 16 & 16 \\ 28 & 14 & 28 & 14 & 16 & 16 & 32 & 16 & 8 & 16 \\ 28 & 14 & 14 & 28 & 16 & 8 & 16 & 32 & 16 & 16 \\ 14 & 28 & 14 & 28 & 16 & 16 & 8 & 16 & 32 & 16 \\ 14 & 14 & 28 & 28 & 8 & 16 & 16 & 16 & 16 & 32 \end{pmatrix},$$

with $\underline{\mu} = (209 - \sqrt{42337}/840) \approx 0.004$ and $\bar{\mu} = (209 + \sqrt{42337}/840) \approx 0.494$, $\bar{\mu}/\underline{\mu} \approx 128$.

REFERENCES

- [1] R. A. Adams, *Sobolev spaces*, Academic Press [A subsidiary of Harcourt Brace Jovanovich, Publishers], New York-London, 1975.
- [2] O. Axelsson and I. Gustafsson, *Preconditioning and two-level multigrid methods of arbitrary degree of approximation*, Math. Comp. **40** (1983), 219–242.
- [3] R. E. Bank, T. F. Dupont, and H. Yserentant, *The hierarchical basis multigrid method*, Numer. Math. **52** (1988), 427–458.
- [4] M. Benzi, G. H. Golub, and J. Liesen, *Numerical solution of saddle point problems*, Acta Numer. **14** (2005), 1–137.
- [5] J. Bey, *Tetrahedral grid refinement*, Computing **55** (1995), 355–378.
- [6] D. Braess and W. Hackbusch, *A new convergence proof for the multigrid method including the V-cycle*, SIAM J. Numer. Anal. **20** (1983), 967–975.
- [7] J. H. Bramble and X. Zhang, *The Analysis of Multigrid Methods*, Handbook of numerical analysis, Vol. VII, North-Holland, 2000.
- [8] S. C. Brenner and L. R. Scott, *The Mathematical Theory of Finite Element Methods*, second ed., Springer-Verlag, 2002.
- [9] P. G. Ciarlet, *Basic error estimates for elliptic problems*, Handbook of Numerical Analysis, Vol. II, North-Holland, 1991.
- [10] H. C. Elman, *Preconditioning for the steady-state Navier-Stokes equations with low viscosity*, SIAM J. Sci. Comput. **20** (1999), 1299–1316.
- [11] A. Ern and J.-L. Guermond, *Theory and Practice of Finite Elements*, Springer-Verlag, 2004.
- [12] V. Girault and P.-A. Raviart, *Finite Element Methods for Navier-Stokes Equations*, Springer-Verlag, 1986.
- [13] W. Hackbusch, *Multigrid Methods and Applications*, Springer-Verlag, 1985.

- [14] J. J. Heys, T. A. Manteuffel, S. F. McCormick, and L. N. Olson, *Algebraic multigrid for higher-order finite elements*, J. Comput. Phys. **204** (2005), 520–532.
- [15] I. C. F. Ipsen, *A note on preconditioning nonsymmetric matrices*, SIAM J. Sci. Comput. **23** (2001), 1050–1051.
- [16] V. John, *Higher order finite element methods and multigrid solvers in a benchmark problem for the 3D Navier-Stokes equations*, Internat. J. Numer. Methods Fluids **40** (2002), 775–798.
- [17] D. Kay, D. Loghin, and A. Wathen, *A preconditioner for the steady-state Navier-Stokes equations*, SIAM J. Sci. Comput. **24** (2002), 237–256.
- [18] M. Marion and R. Temam, *Navier-Stokes Equations: Theory and Approximation*, Handbook of numerical analysis, Vol. VI, North-Holland, 1998.
- [19] M. F. Murphy, G. H. Golub, and A. J. Wathen, *A note on preconditioning for indefinite linear systems*, SIAM J. Sci. Comput. **21** (2000), 1969–1972.
- [20] Y. Saad, *A flexible inner-outer preconditioned GMRES algorithm*, SIAM J. Sci. Comput. **14** (1993), 461–469.
- [21] V. V. Shaidurov, *Multigrid Methods for Finite Elements*, Kluwer Academic Publishers Group, 1995.
- [22] A.D. Stroock, S.K.W. Dertinger, A. Ajdari, I. Mezic, H.A. Stone, and G.M. Whitesides, *Chaotic mixer for microchannels*, Science **295** (2002), 647–651.

DEPARTMENT OF MATHEMATICAL SCIENCES, CHALMERS UNIVERSITY OF TECHNOLOGY, SE-412 96 GÖTEBORG, SWEDEN

E-mail address: erik.svensson@math.chalmers.se